Wind and Structures, Vol. 12, No. 3 (2009) 219-237
DOI: http://dx.doi.org/10.12989/was.2009.12.3.219

Large-eddy simulation and wind tunnel study of flow over an up-hill slope in a complex terrain

C. F. Tsang[1]*, Kenny C. S. Kwok[1,2], Peter A. Hitchcock[1] and Desmond K. K. Hui[3]

[1]CLP Wind/Wave Tunnel Facility, The Hong Kong University of Science and Technology, Hong Kong SAR
[2]School of Engineering, University of Western Sydney, Australia
[3]Transport Department, Hong Kong SAR

(Received March 15, 2008, Accepted March 5, 2009)

Abstract. This study examines the accuracy of large-eddy simulation (LES) to simulate the flow around a large irregular sloping complex terrain. Typically, real built up environments are surrounded by complex terrain geometries with many features. The complex terrain surrounding The Hong Kong University of Science and Technology campus was modelled and the flow over an uphill slope was simulated. The simulated results, including mean velocity profiles and turbulence intensities, were compared with the flow characteristics measured in a wind tunnel model test. Given the size of the domain and the corresponding constraints on the resolution of the simulation, the mean velocity components within the boundary layer flow, especially in the stream-wise direction were found to be reasonably well replicated by the LES. The turbulence intensity values were found to differ from the wind tunnel results in the building recirculation zones, mostly due to the constraints placed on spatial and temporal resolutions. Based on the validated mean velocity profile results, the flow-structure interactions around these buildings and the surrounding terrain were examined.

Keywords: complex terrain; uphill slope; boundary layer; CFD; large eddy simulation.

1. Introduction

In most built up terrains, such as in urban cities, the flow can be very complex. The geometry of buildings, roughness of the surrounding area, varying wind speed and direction, and sloping landscape are all factors which add to the number of variables which affect the flow pattern.

This paper presents the results of a wind tunnel model study and a computational study of wind flow along a steep slope. The flow characteristics, including mean wind velocity and turbulence intensity profiles, were determined by using wind tunnel model test techniques and also a large eddy simulation, with the slope modelled as an irregular step structure. The slope is adjacent to several large buildings, and the effects of these buildings on the flow over the slope were investigated. The measured and computed results are compared to provide validation of the large eddy simulation. The flow-structure interactions around these buildings and the surrounding terrain were examined with a view to future applications, such as pollution dispersion and quantifying topographical effects.

* Corresponding Author, E-mail: wtstsang@ust.hk

2. Flow over complex terrain

A number of studies simulating wind flow over large complex terrain, such as steep slopes and escarpments which are a common topographical feature in Hong Kong, have been conducted. Glanville and Kwok (1997) studied the flow over a steep hill and flow separation at the crest of the hill using wind tunnel models and compared wind tunnel test results with full scale measurements. The results were in good agreement, demonstrating the accuracy of the wind tunnel modelling techniques and tests. The experiments also allowed the determination of topographical multipliers for the steep slope.

The complexity of wind flow over different topographical features has been emphasized in the recent study conducted by Kondo, *et al.* (2002). In that study, the flow characteristics of several slopes with varying gradients were examined and topographic multipliers for different slope gradient angles were established.

In addition to wind tunnel experiments, such as the two studies described above, computational fluid dynamic (CFD) techniques are also commonly employed to study flow over complex terrain. Computationally, studying this type of flow problem is complex and demanding because of the large physical scales involved, which calls for a fine mesh to capture all the significant length scales. This means large computational resources are required, which, considering current technology standards, is often not practical. In order to simplify the problem and allow practical resolution of the Navier Stokes equations, eddy viscosity models were developed, of which one of the most well known is the standard k-epsilon (k-ε) model. However these models have some well known deficiencies, as documented by Murakami (1998).

In recent years, large-eddy simulations (LES) have emerged as an alternative to k-ε type Reynolds averaged Navier-Stokes (RANS) simulations. In LES, the large length scales are simulated directly while the smaller scales are approximated based on a simplified turbulence model. LES can provide valuable information in a spatial and temporal domain, which is necessary for understanding the flow over and around a complex terrain.

All numerical simulations need to be validated, usually through wind tunnel experiments. The importance of validating CFD simulations for engineering applications is discussed thoroughly by Oberkampf and Trucano (2002). That review examines the methods and procedures typically adopted to verify and validate CFD simulations. Currently there is no standard method to verify CFD simulations in an urban environment. This means that simulations need to be rigorously checked to show that they are capable of modelling real world phenomena.

The importance of validation is further emphasized by Castro and Graham (1999) in a paper in which the use of CFD in a wind engineering context was discussed. It emphasised the need for CFD users to have a fundamental understanding of both the basic fluid mechanics of the flow being modelled and also a sound knowledge of the numerical methods employed by the CFD program in order to obtain meaningful results. The importance of validating specific problems and the awareness of the possibility of likely sources of errors were also highlighted by the authors.

A detailed study of a large flat urban terrain was conducted by Tominaga, *et al*. (2004). In that study, several CFD simulations were performed using different software including FLUENT, STAR-CD, and PHOENIX. It was found that most of the revised k-ε models can be used to simulate the velocity profile over an urban terrain, with LES giving the best correlation with wind tunnel experiment values, which would be expected. However, significant differences were found in the results obtained by using different software running the same problem.

A standard k-ε model was used by Hu and Wang (2005) to simulate the flow field around a matrix of cubes located on a flat urban layout. The velocity profile values at street level were found to correlate well with wind tunnel experimental data. However, the results were only valid for a simple geometrical layout. A change in the height of one of the buildings gave poor comparison to measured data. The results highlight the limitations of the standard k-epsilon model when compared to large eddy simulations.

A large urban terrain was also simulated by Skote, *et al.* (2005). Again the terrain was taken as a flat urban terrain and a large city was idealised as large bluff bodies, with the main streets serving as the main airflow channels. The standard k-ε model was used to simulate the flow around the city. Good agreements were reported between the numerical and wind tunnel test results. This was because the city was simplified as large bluff bodies. However, this is not usually the case in real built up areas.

Previous research indicates that most simulations of flow around large urban areas have been conducted on flat urban terrain. The flow around urban areas located on irregular inclined slopes, such as those commonly found in Hong Kong, is worthy of further studies. Additionally, in light of the discussions on the significance of validation studies, the flow over an uphill slope is simulated and the results compared with wind tunnel measurements.

3. Large-Eddy Simulation (LES)

The Navier-Stokes equations govern momentum and energy conservation in a flow regime. The incompressible Navier-Stokes equations written in tensorial notations are:

$$\frac{\partial u_i}{\partial x_i} = 0 \tag{1}$$

and

$$\frac{\partial u_i}{\partial t} + \frac{\partial u_i u_j}{\partial x_j} = \frac{1}{\rho}\frac{\partial p}{\partial x_i} + \nu\frac{\partial^2 u_i}{\partial x_j \partial x_j} \tag{2}$$

where u_i is the velocity component, x_i are the spatial coordinates (i,j=1, 2, 3), p is the pressure, t is the time, ρ is the density and ν is the kinematic viscosity. The problem of turbulence modelling is largely due to the wide variation of turbulence length scales. In order to describe the physical processes adequately, a high grid resolution is needed. This necessitates large amounts of computing power and memory. In addition, a large range of time scales further complicates the problem.

To overcome these problems, various solutions have been proposed including the Reynolds Averaged Navier-Stokes (RANS) solution which gives time-averaged values. These solutions are based on the well known eddy viscosity models. Large-eddy simulations (LES) are another type of approximation where the large turbulence length scales are simulated directly, and the smaller turbulence length scales are calculated based on a simple turbulence model. Numerous texts give a description and explanation of the differences between the LES, direct numerical simulation (DNS) and typical eddy viscosity models such as the k-ε model.

A filter is usually used to separate the large and small scales in the simulation. The small sub-grid scales are treated using the Smagorinsky-Lilly form of the LES, which is a viscosity model based on the Boussinesq approximation. To obtain the equations for the LES, the Navier-Stokes equations are filtered using the following equation:

$$\bar{f}(r,t) = \int_V G(|r-r'|)f(r',t)dr' \quad (3)$$

In Eq. (3), $\bar{f}$ represents the filtered variable $f(x_i, t)$ and $G(|x - x_i'|)$ is the filter function. The most common type of filter is the following box filter:

$$G(x - x_i') = \begin{cases} \frac{1}{\Delta_i} \text{ if } |x_i - x_i'| \le \frac{\Delta_i}{2}, \text{ otherwise is } 0 \end{cases} \quad (4)$$

The filter width Δ_i separates the length scales into large resolved and smaller sub-grid scales. Through the filtering process, the Navier-Stokes equations are transformed into the following form:

$$\frac{\partial \bar{u}_i}{\partial x_i} = 0 \quad (5)$$

and

$$\frac{\partial \bar{u}_i}{\partial t} + \frac{\partial \bar{u}_i \bar{u}_j}{\partial x_j} = \frac{1}{\rho}\frac{\partial \bar{p}}{\partial x_i} + \upsilon \frac{\partial^2 \bar{u}_i}{\partial x_j \partial x_j} - \frac{\partial \tau_{ij}}{\partial x_i} \quad (6)$$

$\bar{u}_i$ and $\bar{u}_j$ are the resolved scale velocity vectors in the x_i and x_j directions. $\bar{p}$ is the resolved pressure. The sub-grid scales Reynolds stresses are given by τ_{ij}.

$$\tau_{ij} = \overline{u_i u_j} - \bar{u}_i \bar{u}_j \quad (7)$$

The small scale grid stresses relate the resolved grid stresses to the unresolved sub-grid scales. This is modelled using the eddy viscosity model in which it is assumed that the sub-grid scale stresses are proportional to the strain rate tensor as follows.

$$\tau_{ij} - \frac{1}{3}\delta_{ij}\tau_{kk} = -2\nu_T \bar{S}_{ij} = -2C\Delta^2 |\bar{S}| \bar{S}_{ij} \quad (8)$$

where $\bar{S}_{ij}$ is the resolved scale strain rate tensor,

$$\bar{S}_{ij} = \frac{1}{2}\left(\frac{\partial \bar{u}_i}{\partial \chi_j} + \frac{\partial \bar{u}_j}{\partial \chi_i}\right) \quad (9)$$

δ_{ij} is the Kroneker delta, ν_T is the sub-grid scale eddy viscosity. Δ is the length scale and is equal to $(\Delta x_1 \Delta x_2 \Delta x_3)^{0.3}$, where Δx_i denotes the grid spacing. $|\bar{S}| = \sqrt{2\bar{S}_{ij}\bar{S}_{ij}}$ is the magnitude of the strain tensor. C is the Smagorinsky constant and is taken as 0.1 in FLUENT, which is the software used in the current study.

4. Flow over a complex terrain - test site, wind tunnel test and computational study

4.1. Test site

The Hong Kong University of Science and Technology (HKUST) is situated on the east coast of Kowloon amidst complex terrain. Campus buildings are generally medium-rise, i.e. of the order of 8

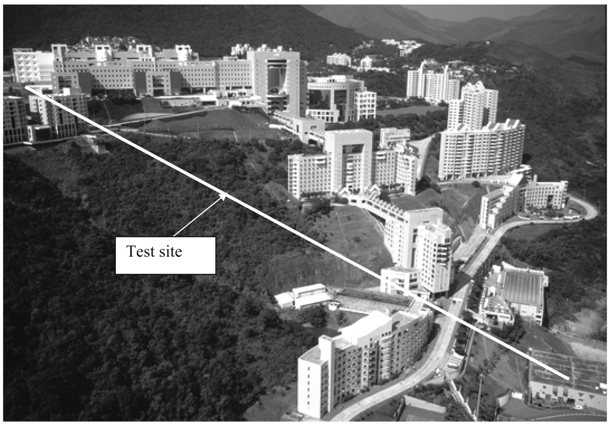

Fig. 1 Topography at the Hong Kong University of Science and Technology

- 12 storeys, that provide accommodation to staff and students and teaching and laboratory facilities. The test site, as shown in Fig. 1, is located on a hillside that extends from the waterfront to an elevation of approximately 120 m above sea level. A number of medium-rise buildings are scattered along the hillside. The site is exposed to a wide range of climate systems and is regularly impacted upon by strong north-east monsoons and typhoons.

4.2. Wind tunnel test of flow over a complex terrain

The characteristics of wind flow approaching the test site were first studied in a 1:2000 scale topographical model test conducted at the CLP Power Wind/Wave Tunnel Facility (WWTF), as shown in Fig. 2. Measured mean wind velocity and turbulence intensity profiles were then simulated at 1:400 scale using roughness elements and wooden fences to study the flow field over the test site in greater detail. A 1:400 scale model was fabricated of the test site and topography within a distance of approximately 500 m from the centre of the site. Terrain roughness in the test

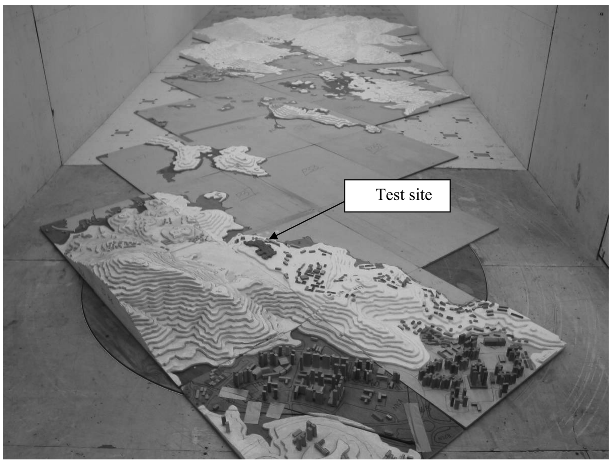

Fig. 2 1:2000 Scale model of Hong Kong University of Science and Technology model was reproduced at 4 m contour intervals, creating a terraced effect, upon which the various building block models were mounted, and is shown in Fig. 3. This is described in detail in the report by Hitchcock, *et al.* (2006).

Time histories of the three components of wind velocity were measured by two Cobra probes along the centre line of the wind tunnel at distances 3.5 m and 1.75 m upstream of the centre of the 1:400 scale model. Additional velocity time histories were measured along three longitudinal vertical planes, offset laterally from the centre of the model by +75 mm, 0 mm and -75 mm, denoted as measurement planes A, B and C respectively in Fig. 4, to compare with CFD predictions. Statistical and spectral analyses of the measured wind velocities were carried out to deduce the total turbulence intensity and turbulence length scale respectively.

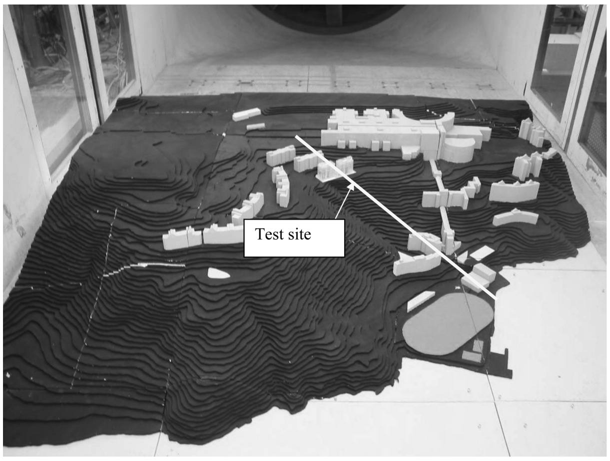

Fig. 3 1:400 Scale model of the Hong Kong University of Science and Technology

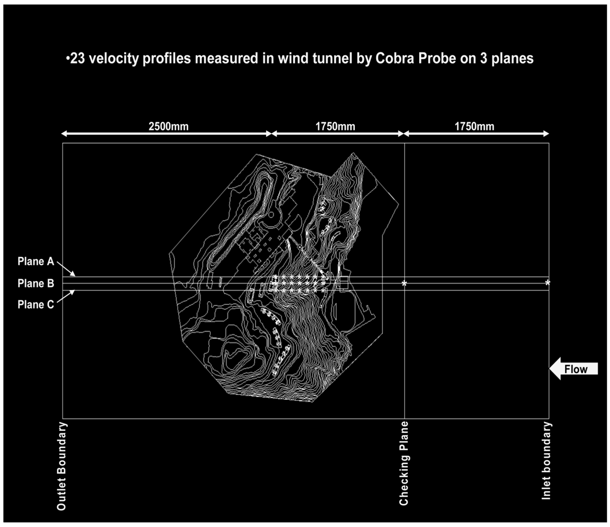

Fig. 4 Location of three longitudinal planes and measuring points

4.3. Computational model for flow over a complex terrain

The computational domain together with the location of the origin is shown in Fig. 5. The size of the computational domain simulated is 6 m × 3 m × 2 m. Fig. 6 shows the inlet and outlet plane with the three measurement planes A, B and C at x = 1.454, 1.529 and 1.604 m. The sloping terrain consists of a stepped structure, and a structured mesh, as shown in Fig. 6, was used to model the terrain. The mesh consisted of 2.96 million volumes. The near wall treatment was used to resolve the flow close to the surface.

Profiles of mean wind speed and turbulence intensity simulated at 1:400 scale were based on measurements taken at heights equivalent to 30, 50, 75, 100, 139, 200 and 300 m above Hong Kong Principal Datum (mPD) at prototype scale. 139 mPD is the height of the buildings at the top of the slope. Inlet boundary conditions were simulated by taking these measurements of mean inlet

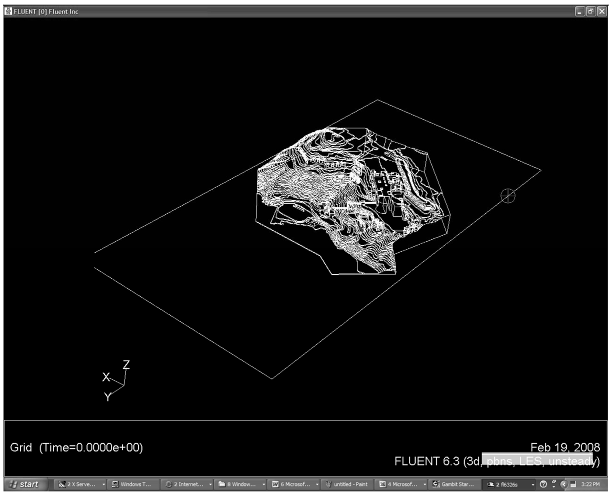

Fig. 5 Computational domain and location of origin

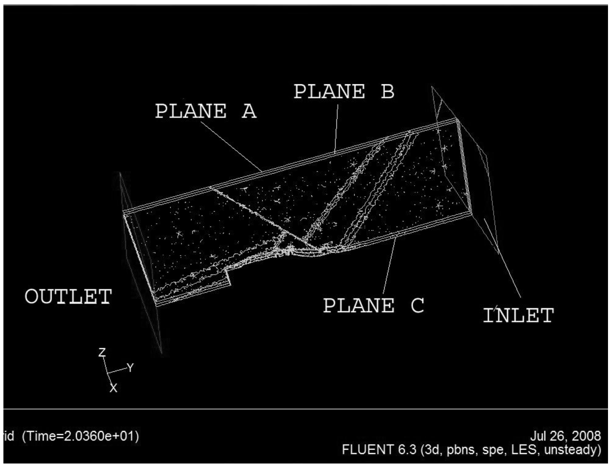

Fig. 6 Inlet and outlet planes and measurement planes A, B and C

velocity and turbulence from the wind tunnel test and then using these values to calculate an artificial fluctuating velocity using the technique outlined by Smirnov, *et al.* (2001). The outlet was assigned with zero diffusion flux flow, so that the outflow velocity and pressure are consistent with a fully developed flow assumption, i.e.

$$\frac{\partial p'}{\partial x_n} = 0 \tag{10}$$

The surface of the whole model was assigned with a no slip wall boundary, where the normal velocity component was set to zero. The time simulated was 20 s at a time step of 0.04 s. A computer system consisting of eight parallel PCs was used to perform the simulation. The finite volume method for discretizing the Navier-Stokes equation was utilised by FLUENT.

5. Results and discussion

5.1. Mean velocity

The longitudinal, lateral and vertical profiles determined from the wind tunnel and simulation results along measurement planes A, B and C are shown in Figs. 7 to 9 respectively. The results indicate some variations in the correlation between computed and measured results of the flow along the three planes studied. The variations for the lateral velocity component and vertical velocity component are generally larger than those found in the longitudinal velocity component and, of the three measurement planes, plane C gives the closest agreement to the wind tunnel test results for all three velocity components.

The longitudinal component of velocity shows the best correlation between the computed and wind tunnel test results. This component of velocity is in the stream-wise direction, which is typically the most important amongst the three velocity components for wind engineering applications. The longitudinal velocity profile characteristics are generally well modelled by the simulation, with only small differences between the computed and measured profiles. There are good agreements even close to the wall boundaries where the accuracy is expected to be more significantly affected by the mesh resolution. The near wall mesh resolution is typically a function of Re^3, which means that an increasing amount of computing resources in relation to the Reynolds number of the flow is theoretically required as mentioned by Leschziner (2003). The mesh should be more fine in the areas which have rapid changes in velocity. This would include the flow direction and the flow around the building areas.

Examination of the local ground profiles shows that there are large buildings close to the bottom of the slope along planes A and B, at $y = 2.245$ m, $y = 2.145$ m with the plane C relatively unaffected. Although the spatial resolution may not have been able to fully capture the flow separation expected to occur behind the buildings, hence resulting in a distortion of the upstream velocity profile, there are still good agreements between simulated and measured velocity profiles further along the slope downstream of the buildings.

The computed longitudinal velocity profiles at the boundary layer close to the surface, which have been modelled using the near wall treatment as opposed to the log law wall profile, also show good similarity to the wind tunnel test results.

Figs. 10 and 11 show the velocity vectors around two buildings at the downstream ends of the slope along planes A and C. The computed flow pattern clearly shows the stagnation points on the

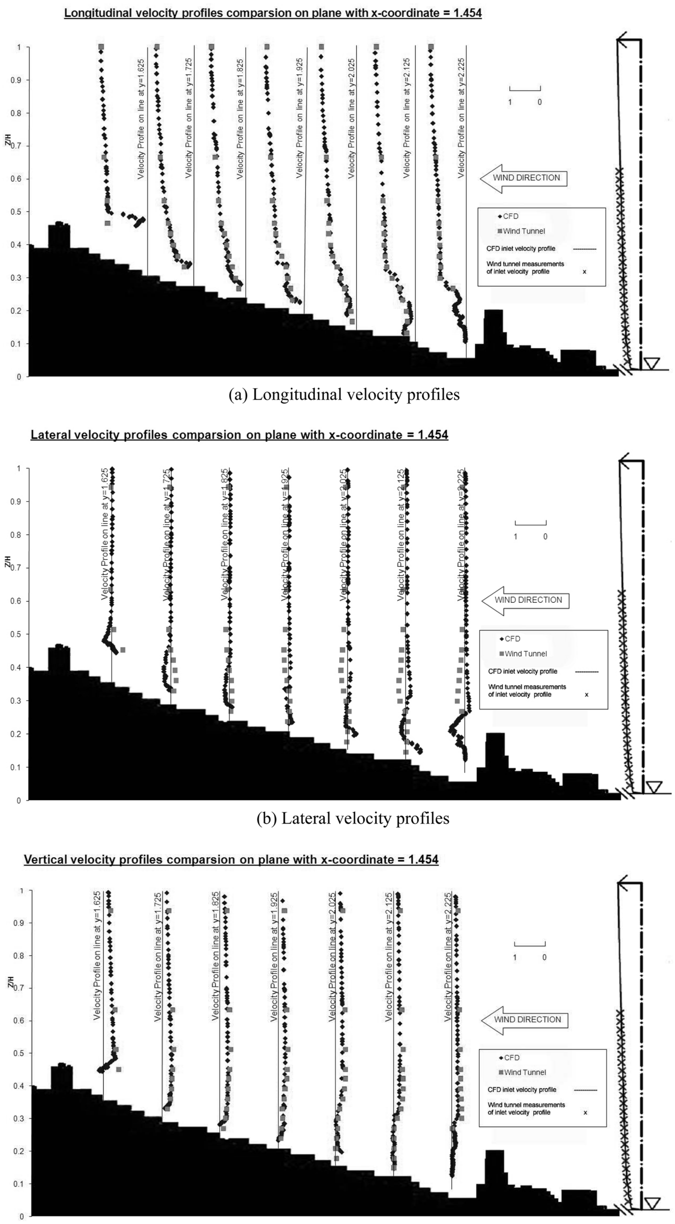

(a) Longitudinal velocity profiles

(b) Lateral velocity profiles

(c) Vertical velocity profiles

Fig. 7 Mean velocity profiles along plane A

windward faces, flow separations at the windward edges of the roofs and flow recirculation behind the buildings. This indicates that the important characteristics of the flow over the buildings have been well simulated. This, coupled with the agreements presented earlier between the computed and wind tunnel test results of velocity profiles along the slope, reinforces the ability of the computational model adopted to simulate the flow along an inclined slope within a complex terrain.

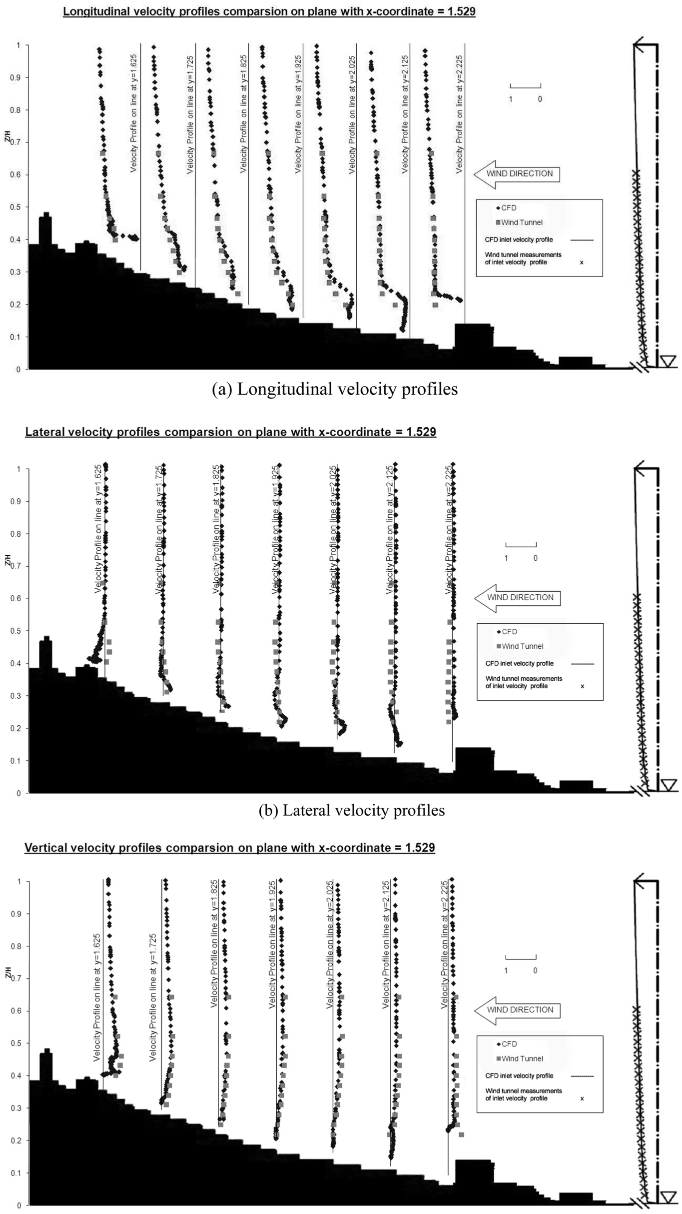

(a) Longitudinal velocity profiles

(b) Lateral velocity profiles

(c) Vertical velocity profiles

Fig. 8 Mean velocity profiles along plane B

5.2. Turbulence intensity

Turbulence intensity is a measure of the magnitude of the fluctuating wind component compared to the mean wind speed at the same height z. The computed and wind tunnel measured total turbulence intensities are shown in Figs. 12 to 14. Comparisons between the computed and wind tunnel test results tend to be better away from the surface of the slope and on the upper part of the

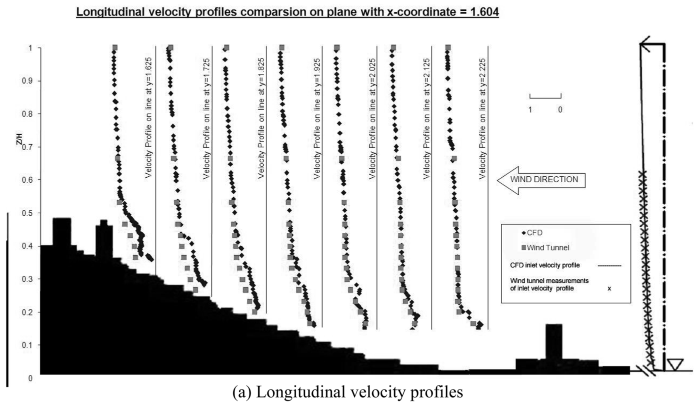

(a) Longitudinal velocity profiles

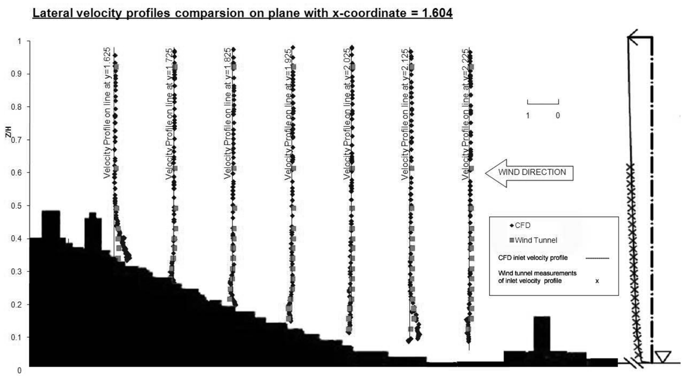

(b) Lateral velocity profiles

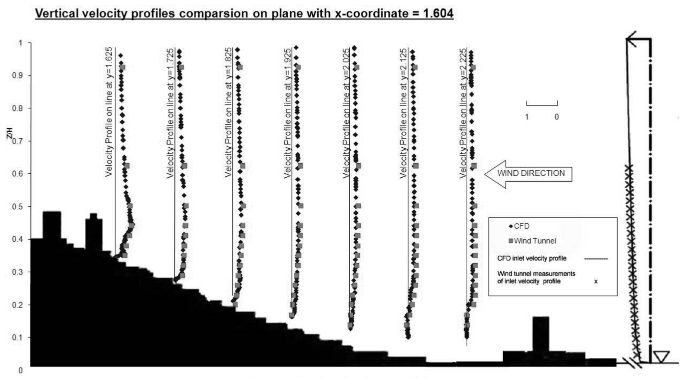

(c) Vertical velocity profiles

Fig. 9 Mean velocity profiles along plane C

slope away from the building recirculation zones. For example, the computed and measured turbulence intensities are within 5% for all three planes at y = 1.625 m. At y = 1.725 m, the variations range from 5% to 30% with higher deviations from wind tunnel measurements occurring at the surface. For the case of y = 1.825m, the variations are around 5% to 40%, again with the larger differences occurring close to the ground level. For points lower down the slope, the computed results deviated from the wind tunnel results by greater amounts due to the recirculating flow. It is important to note that at the bottom of the slope and behind the buildings the turbulence intensity calculated by the simulation which exceeded 100% has been omitted. This is used to

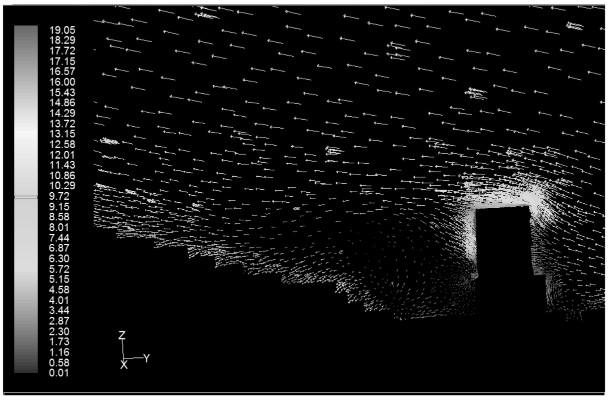

Fig. 10 Velocity vectors at bottom of the slope at plane A

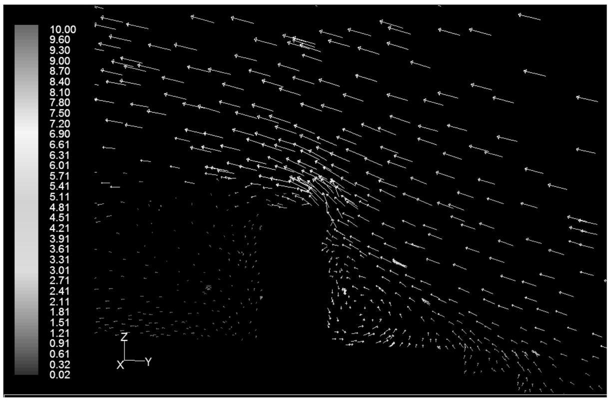

Fig. 11 Velocity vectors at bottom of the slope at plane C

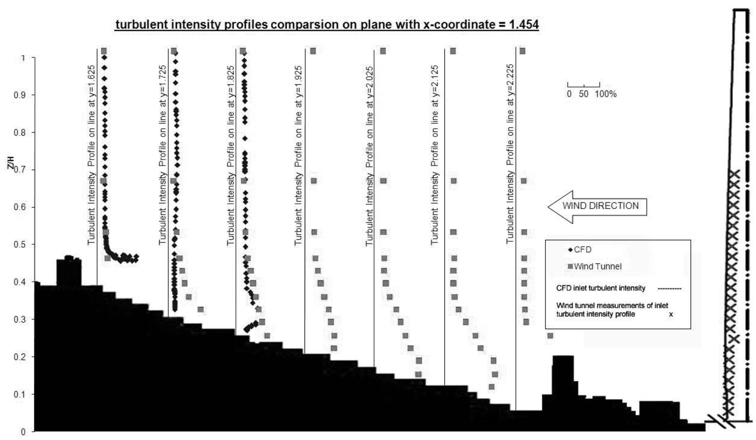

Fig. 12 Comparison of turbulence intensity results along plane A

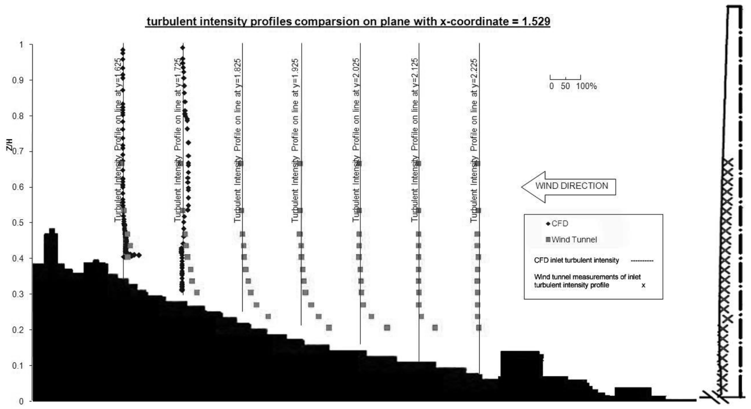

Fig. 13 Comparison of longitudinal turbulence intensity results along plane B

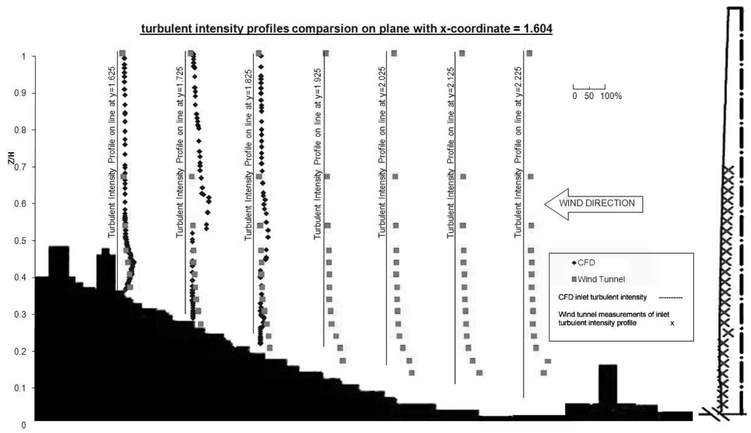

Fig. 14 Comparison of turbulence intensity results along plane C

illustrate the point that the large eddy simulation is unable to model the recirculation zone behind the building. However at the top of the slope away from the recirculation zone the turbulence intensity is well modelled.

Generally, the turbulence values determined from the CFD model are underestimated close to the ground surface and overestimated at the bottom of the slope closer to the building recirculation zones. Again, it was found that plane C gave better correlations between computed and measured results in comparison to planes A and B. This is attributable to the building at the bottom of the slope being further upstream for plane C, with a corresponding lowering in the turbulence shed from the building. At locations adjoining the slope and the buildings, a particularly fine mesh is required to show all the length and time scales of the flow.

In addition to the discrepancies associated with the meshing scheme, there are other important contributing factors. The first factor relates to the eddy sub-grid scale stress models. The behaviour of these models and their dependencies on the Smargorinsky constant have been discussed by Deardoff (1971). This means that close to wall surfaces, where the anisotropic behaviour becomes significant, the accuracy of the model deteriorates. As a means of compensation, it has been suggested that value of the Smagorinsky constant should vary at different locations, Canuto and

Cheng (1997). To obtain improved results, it would be better to conduct the simulation using a dynamic sub-grid scale model, where the Smagorinsky constant varies with time and location. However, this may lead to problems of instability for flow past bluff bodies, as mentioned by Murakami and Izuki (1999).

Secondly, significant errors are likely to be introduced due to the low temporal resolution of the large eddy simulation. The time step of 0.04 s seems small but even at this resolution it is not enough to capture the entire time history of the velocity fluctuations. This is especially important behind the building where there is highly turbulent flow. The calculation of the turbulence intensities is given by

$$I_{u_{i,Z}} = {}^{\sigma}u_{i,Z}/U_Z \tag{11}$$

The standard deviation σ is given by

$$\sigma_{ui,z} = \sqrt{\frac{1}{T}\int_0^T [u_z(t)]^2 dt} \tag{12}$$

where i = 1, 2 and 3 directions represent the velocity components. If there are insufficient time steps, not all the length scales are properly simulated, resulting in erroneous turbulence intensity values.

It should be noted that, given sufficient resolution, the large eddy simulation should be able to reproduce satisfactorily the turbulence intensity profiles measured in the wind tunnel model. In the research conducted by Maruyama, *et al.* (1999), a LES of a high Reynolds number flow over a rough surface boundary layer was simulated. The simulated turbulent flow was compared with experimental data and found to give good agreement. In a more recent study conducted by Tutar and Oguz (2002), the flow between two parallel buildings was simulated. The accuracy of the simulated turbulent kinetic energy calculated by several RANS and LES models was assessed. It was found that LES with sub-grid scale models gives superior simulated results compared to RANS in relation to wind tunnel measurement data.

High resolution means that the main characteristics of the flow structure are numerically simulated by the Navier-Stokes equations and are not significantly affected by the sub-grid scale model. The finer the grid, the more of the flow is actually simulated and less is resolved using the simplified eddy viscosity turbulence models. The major objective of this study was to examine the entire flow of a large complex terrain. Consequently, the available computational resources were necessarily spread over a large area, balancing area coverage against using a finer grid closer to the ground surface, which would have significantly improved the simulation accuracy. Furthermore, many topographical features upstream and downstream of the slope can affect the flow over the test site. Hence the entire slope face and all surrounding buildings have to be included in the simulation domain. Overall, the ability of the computational model to simulate the mean flow over a large complex terrain can facilitate the investigation of problems such as pollution dispersion over a large area, or where the overall flow pattern is the main objective.

The accuracy of the large-eddy simulation depends on the combination of available computational power and the Reynolds number of the flow and the complexity of the flow. In this case the complex terrain results in more complex flow characteristics because of the upward sloping incline and buildings which means more additional computational resources are required.

5.3. Computer requirements for large-eddy simulations

Large-eddy simulations require a large amount of compuational resources in comparison to two equation eddy viscosity models, as highlighted by many researchers such as Mochida (2008) and Lubcke, *et al.* (2001) . The use of coarse grids for large eddy simulations will result in the increase of numerical discretisation errors, as recently reported by Raufeisen, *et al.* (2009). In the case of complex terrain, the more complex flow patterns arising from more rapid changes in velocity due to the uneven ground surface and building arrangements means that the computational resources required are even larger. However, future increases in computing power should eventually allow large eddy simulations to overcome many of the limitations associated with current computer technology. For this study, all available computer resources were utilised in the simulation.

5.4. Sensitivity analysis

The importance of performing sensitivity analyses for large eddy simulations in wind engineering applications should also be emphasized, particularly for the accuracy of the simulation results, such as velocity and pressure, in response to changes in domain and boundary conditions such as inlet velocity, incidence angle, kinetic energy, turbulent viscosity, y+ (distance of first grid point to the boundary surface) values. The lack of detailed studies reported in the literature and the complexity of the problem of sensitivity ananlysis for large eddy simulations has recently been reported by Meyers, *et al.* (2008). Sensitivity analysis was also identified by Huang and Jacob (1998) as one of the validation criteria for all turbulence models. For the simulation conducted in the current study, the results were checked for changes in inlet velocity and turbulent viscosity, demonstrating similarity in both the flow structures and velocity vectors, but with higher velocity magnitudes as would be expected with flow of equal Reynolds number.

5.5. Effects of buildings on mean velocity profiles

Based on the above validation of the mean velocity, the effect of the buildings on the development of the velocity profiles along the hillside is discussed. The topographical profiles of the three measurement planes considered in this study, including the location of the buildings, are shown in Figs. 15 to 17.

The velocity vectors shown in Figs. 15 to 17 give a good indication of the stagnation points on the windward faces, flow separations at the windward edges of the roofs and flow recirculation behind and in between the buildings. Large recirculation zones can be observed behind all the large buildings along the three measurement planes. The recirculation area overlaps slightly onto the start of the slope for planes A and B, making the flow more turbulent, slightly disrupting the flow up the slope up to a distance of approximately a quarter of the length of the slope. Generally, the mean longitudinal velocity is reduced by about 50% close to the ground surface in these recirculation zones. Along plane C, the downstream building is further away from the crest of the hillside and the effect is smaller. Figs. 15 and 16 also show that the velocities up the slopes are more disrupted by the slightly taller buildings located at the downstream end of planes A and B.

Recirculation in the flow between the three buildings at the top of the slope at plane C can also be clearly seen in Fig. 18. The air between the buildings is trapped, resulting in a largely stagnant zone. This air entrapment is typical of built up areas with closely spaced buildings and can lead to

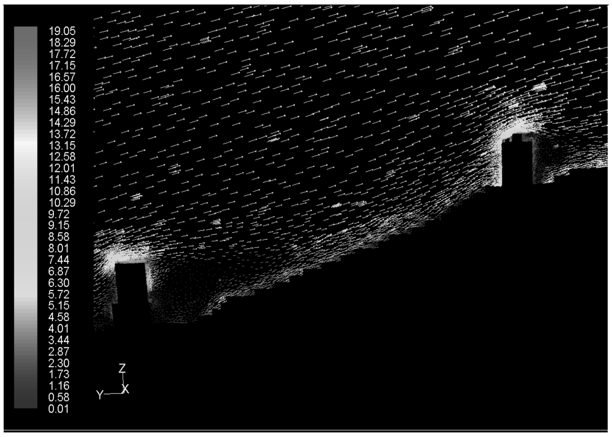

Fig. 15 Velocity vectors along slope along plane A

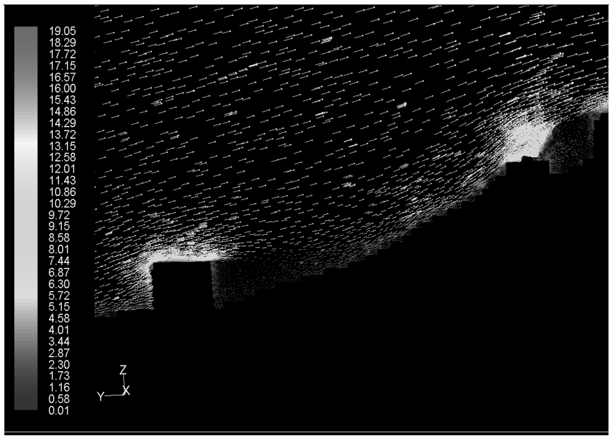

Fig. 16 Velocity vectors along slope along plane B

Fig. 17 Velocity vectors along slope along plane C

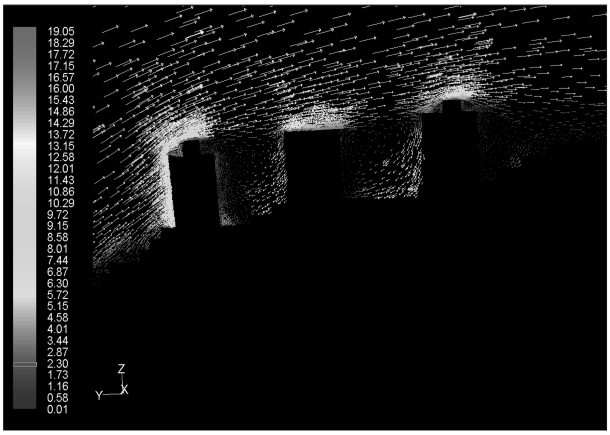

Fig. 18 Velocity vectors around three buildings at the top of slope at plane C

areas of poor ventilation. The Cobra probe used in the current study was unable to accurately measure the flows between the buildings to extract meaningful validation data for this area, although the simulated flow pattern is consistent with descriptions from previous studies of ventilation in street canyons, such as the study by Xie, *et al.* (2006).

In Fig. 10, the simulation illustrates the streamwise airflow at plane A moving over the top of the building at the bottom of the slope, then losing momentum due to the presence of the building. A large, highly turbulent flow recirculation zone then forms immediately behind the building. However, as the flow passes the large bluff body, it begins to regain momentum. A smoother velocity profile then forms further downstream of the building. The transfer of the flow over the building and onto the slope has been well simulated. Although the turbulence behind the building has not been well reproduced, the velocity of flow over the building and onto the slope has shown good correlation with the wind tunnel experiments. This means that the simulation shows potential to be used to determine pollution transportation around complex terrains and buildings, in terms of flow separation and reattachment.

In the current study, the presence of buildings has been simulated, but the simulation can equally be well run without buildings. This facilitates the determination of topographical multipliers associated with various topographical features with and without the presence of buildings and other built structures. The present validation of LES can form the basis for future studies in topographical modelling and pollution dispersion studies.

6. CONCLUSIONS

The correlation between computed and wind tunnel test results indicate that the mean velocity profile in the streamwise direction of the flow uphill in a complex terrain can be adequately modelled by LES utilising limited computing resources. The use of the near wall treatment for simulating the boundary layer close to the surface has been shown to yield satisfactory results.

The turbulence intensity was less well modelled in areas near the surface of the slope and behind the buildings. This is mainly attributable to the limited computational resources and the inadequacies of the eddy viscosity sub-grid scale models. Evidently, a large amount of memory and processing power is required for large eddy simulation to accurately simulate the flow over the many topographical features in a complex terrain and the resultant flow patterns. Given adequate computer memory and processing power, it is expected that the turbulence structure can also be modelled more satisfactorily.

The wind velocity vectors produced by the LES have also been used to study the flow-structure interaction between the buildings and the surrounding terrain along the uphill slope. The simulated flow patterns reproduced the expected stagnation zone on the windward faces of the buildings, flow separations at the windward edges of the roofs and flow recirculation between and behind the buildings

In practice, urban environments may consist of complex geographical features like the one simulated in this study. The study has shown that even with limited computational facilities, the mean velocity profile along a steep slope in a complex terrain with varying geographical features and buildings can be reasonably well modelled by the large eddy simulation. The correlations between computed and wind tunnel measured mean velocity values indicate good overall accuracy of the simulation in the entire computational domain. Hence CFD, when properly validated, has the potential to provide an alternative and/or complementary tool to wind tunnel tests in the study of wind-structure interactions in urban environments.

Acknowledgements

This research is supported by the Research Grants Council of Hong Kong (Project: HKUST 6293/03E).

References

Canuto, V.M. and Cheng, Y. (1997), "Determination of the Smagorinsky–Lilly constant CS", *Phys. Fluids*, **9**, 1368-1378.

Castro, I. and Graham, J.M.R. (1999), "Numerical Wind Engineering, the way ahead?", *Proc. of Institute of Civil Engineers*, *Struct. Build.* , **134**(3), 275-277.

Deardorff, J.W. (1971), "On the magnitude of the subgrid-scale eddy coefficient", *J. Comput. Phys.*, **7,** 120-133.

Glanville, M.J. and Kwok, K.C.S. (1997), "Measurements of topographic multipliers and flow separation from a steep escarpment. Part II Model measurements", *J. Wind Eng. Ind. Aerod*., **69-71**, 893-902.

Hitchcock, P.A., Campbell, S., Hui, D.K.K., Thepmongkorn, S. and Kwok, K.C.S. (2006), "External wind pressures for a Hong Kong apartment building - wind tunnel test results", *Proc. of 12th AWES Wind Engineering workshop*, Queenstown, New Zealand.

Hu, C.H. and Wang, F. (2005), "Using a CFD approach for the study of street-level winds in a built-up area", *Build. Environ.*, **40**(5), 617-631.

Huang, P.G. and Jacob, J.D. (1998), "On the development of an intelligent code validation system for the rapid transfer of turbulence model technology", *Proc. of Fluids Engineering Division Summer Meeting*, *ASME Fluids Engineering division Summer meeting*, June 21-25, 1-8.

Kondo, K., Tscuchiya, T. and Sanada, S. (2002), "Evaluation of effect on micro-topography on design wind velocity", *J. Wind Eng. Ind. Aerod*., **90**, 1707-1718.

Leschziner, M.A. (2003), "Computational modelling of complex turbulent flow-expectations, reality and prospects", *J. Wind Eng. Ind. Aerod*., **46-47**, 37-51.

Lubcke, H., Schmidt, S., Rung, T. and Thiele, F. (2001), "Comparison of LES and RANS in bluff-body flows", *J. Wind Eng. Ind. Aerod*., **89**, 1471-1485.

Maruyama, T., Rodi, W., Maruyama, Y. and Hiraoka, H. (1999), "Large eddy simulation of the turbulent boundary layer behind roughness elements using an artificially generated flow", *J. Wind Eng. Ind. Aerod*., **83**, 381-392.

Meyers, J., Geurts, B.J. and Sagaut, P. (2008), *Quality and Reliability of Large-Eddy Simulation*, **12**,

ERCOFTAC Series, Springer Netherlands, Netherlands.
Mochida, A., Lun, I. (2008), "Prediction of Wind environment and Thermal comfort at Pedestrian level in urban area", *J. Wind Eng. Ind. Aerod*., **96**, 1498-1527.
Murakami, S. (1998), "Overview of turbulence models applied in CWE–1997", *J. Wind Eng. Ind. Aerod*., **74-76**, 1-24.
Murakami, S. and Izuki, S. (1999), "CFD analysis of turbulent flow past a square cylinder using dynamic LES", *J. Fluids Struct.*, **13**, 1097-1112.
Oberkampf, W.L. and Trucano, T.G. (2002), "Verification and validation in computational fluid dynamics", *Prog. Aerosp. Sci.*, **38**(3), 209-272.
Raufeisen, A., Breuer, M., Botsch, T. and Delgado, A. (2009), "LES validation of turbulent rotating buoyancy– and surface tension–driven flow against DNS", *Comput. Fluids*, doi: 10.1016/j.compfluid.2009.01.002 *(in press)*.
Skote, M., Sandberg, M., Westerberg, U., Claesson, L. and Johansson, A.V. (2005), "Numerical and experimental studies of wind environment in an urban morphology", *Atmos. Environ.*, **39**(33), 6147-6158.
Smirnov, A., Shi, S. and Celik, I. (2001), "Random flow generation technique for Large Eddy Simulations and particle dynamic modelling", *J. Fluids Eng.*, **123**, 359-371.
Tominaga, Y., Mochida, A., Shirasawa, T., Yoshie, R., Kataoka, H., Harimoto, K. and Nozu, T. (2004), "Cross comparison of CFD results of wind environment at pedestrian level around a high rise building and within a building complex" , *J. Asian architect. Build. Eng*., **3**(1) , 63-70.
Tominaga, Y., Mochida, A., Yoshie, R., Kataoka, H., Tsuyoshi, N., Masaru, Y. and Taichi, S. (2008), "AIJ guidelines for practical applications of CFD to pedestrian wind environment around buildings", *J. Wind Eng. Ind. Aerod*., **96**, 1749-1761.
Tutar, M. and Oguz, G. (2002), "Large eddy simulation of wind flow around parallel buildings with varying configurations", *Fluid Dyn. Res.*, **31**, 289-315.
Xie, X., Huang, Z. and Wang, J. (2006), "The impact of urban street layout on local atmospheric environment", *Build. Environ.*, **41**, 1352-1363.

JH